Proceeding Paper

COVID-19 Lung Radiography Segmentation by Means of Multiphase Transfer Learning †

Plácido L. Vidal [1,2,*] 📵 , **Joaquim de Moura** [1,2] 📵 , **Jorge Novo** [1,2] 📵 and **Marcos Ortega** [1,2] 📵

1   Centro de investigación CITIC, Universidade da Coruña, Campus de Elviña, s/n, 15071 A Coruña, Spain; joaquim.demoura@udc.es (J.d.M.); jnovo@udc.es (J.N.); mortega@udc.es (M.O.)
2   Grupo VARPA, Instituto de Investigación Biomédica de A Coruña (INIBIC), Universidade da Coruña, Xubias de Arriba, 84, 15006 A Coruña, Spain
*   Correspondence: placido.francisco.lizancos.vidal@udc.es
†   Presented at the 4th XoveTIC Conference, A Coruña, Spain, 7–8 October 2021.

Abstract: COVID-19 is characterized by its impact on the respiratory system and, during the global outbreak of 2020, specific protocols had to be designed to contain its spread within hospitals. This required the use of portable X-ray devices that allow for a greater flexibility in terms of their arrangement in rooms not specifically designed for such purpose. However, their poor image quality, together with the subjectivity of the expert, can hinder the diagnosis process. Therefore, the use of automatic methodologies is advised. Even so, their development is challenging due to the scarcity of available samples. For this reason, we present a COVID-19-specific methodology able to segment these portable chest radiographs with a reduced number of samples via multiple transfer learning phases. This allows us to extract knowledge from two related fields and obtain a robust methodology with limited data from the target domain. Our proposal aims to help both experts and other computer-aided diagnosis systems to focus their attention on the region of interest, ignoring unrelated information.

Keywords: CAD system; radiography; X-ray; lung segmentation; COVID-19; transfer learning

1. Introduction

In 2020, a new variant of coronavirus spread around the world, known as SARS-CoV-2. This variant, which causes the COVID-19 pathology, is known to cause a viral pneumonia and severe acute respiratory syndrome as its main symptoms. Due to the aerosol transmission capabilities of the virus and the possibility of contagion through surfaces, specific protocols and independent circuits were designed in the health services in order to avoid cross-contamination between hospital personnel and patients. Chest X-rays and computerized tomography scans are mainly used to diagnose this pathology in order to determine the degree of the affliction of the patients, which allows us to see the state of the lungs in a non-invasive way. However, this medical imaging equipment is usually set up in rooms specifically designed for them, with certain safety measures. For this reason, to prevent said cross-contamination, the use of portable X-ray devices that can be used in these alternative circuits is recommended. On the other hand, these devices only allow a limited range of planes from which images of the patient can be extracted. Moreover, due to their nature, the images tend to be of lesser quality. These two factors, together with the emergency situation and the inherent subjectivity of a human expert, can result in challenges in making a quick, correct and repeatable diagnosis for further monitoring of the afflicted. It is precisely for this reason that the use of computer-based diagnostic support systems to assist in the task is necessary.

The main problem that emerged in the development of these methodologies derives from the scarcity of available samples due to the exceptionality of the scenario as well as the target domain. For this reason, methodologies were developed based on the prominent

classical lung radiographs from fixed devices [1,2]. Even so, the results from these automatic methodologies were not as accurate as would be desired, as they were unprepared to work with these portable devices. This way, there were attempts to develop both methodologies trained with a reduced dataset with networks robust to this data scarcity [3], methodologies that proposed generating synthetic samples from zero to train more powerful networks weak to this data scarcity [4] and, like in the work proposed here, methodologies that aim to assist both clinicians and other computer-aided diagnosis systems by reducing the presence of extraneous elements [5]: a robust lung segmentation strategy for chest radiographs from portable devices.

2. Materials and Methods

For the development of our proposal we employed three different domains represented in Figure 1. Using as baseline brain magnetic resonance images for glioma segmentation, we took advantage of a pretrained U-Net model from the work of *Buda* [6]. These pathological bodies (and also natural structures present in the image) show similar gradient and texture patterns as lung regions afflicted by different respiratory tract diseases. The second domain consists in chest radiographs that were obtained with classical X-ray devices [7,8] to further approximate the deep features of the network to the target images from portable devices (introducing it to the patterns of the target organ and pathology). Finally, the third (and target) domain is composed of images that were captured during live clinical practice from a local hospital during the COVID-19 pandemic (the Universitary Hospital Complex of A Coruña or CHUAC, by its acronym in Spanish) with portable chest X-ray devices. To ensure that the system would be able to properly perform in a real clinical scenario in even the most borderline cases, both chest radiography datasets include both COVID-19 and healthy patients, but also a third class of pathological lung radiographs with a similar profile as patients with COVID-19 (but not being actually afflicted by it). These scenarios mainly include similar cases of viral and bacterial pneumonia that leave a very similar trace in the chest radiographs.
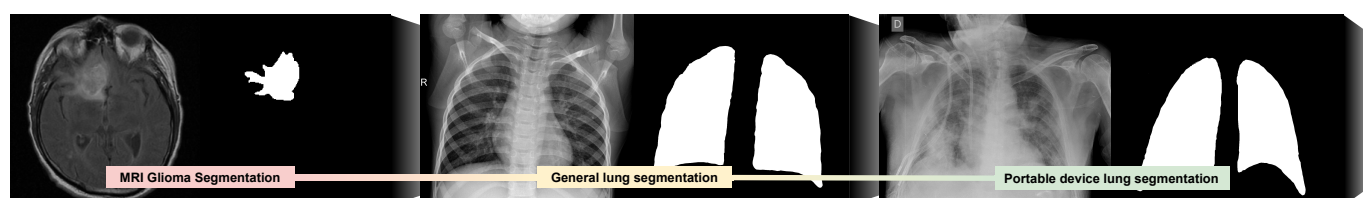

Figure 1. Representation in order of the three domains from which we will perform the knowledge transfer.

This way, we first adapt the classification layer of the U-Net pretrained with glioma images dataset and resume the training with the general lung radiographs. This allows the network to learn to segment these radiographs in a reduced number of epochs. Afterwards, we further refine the classification of this model by resuming the training, but now with images from our dataset composed by chest radiographs from portable devices.

3. Results and Discussion

The results attained in both transfer learning stages can be seen in Table 1. In both cases, the results are shown with the same independent dataset with images that were extracted by means of portable X-ray devices. As we can see, the results that were obtained by the system are satisfactory with all the studied metrics. However, we see two metrics that clearly stand out from the rest after the second phase of transfer learning: the Dice and the sensitivity that improve by 0.0688 and 0.0804 on average in the three classes, respectively. These metrics indicate that, while in both cases the system was able to obtain an approximate segmentation to the lung region, after the second phase of knowledge transfer these segmentations are more adjusted to the regions of interest established by the experts (even despite the aforementioned deterioration in image quality and limitations).

For this reason, we can see that, in fact, we have obtained a more robust system compared to those trained only with classical lung radiographs thanks to the progressive adaptation of the latent features of the network, and only needing a reduced number of samples.

Table 1. Test results from the inter domain (a) and inter device type (b) knowledge transfer phases.

(a)			
	COVID-19	**Normal**	**Pathological**
Accuracy	0.9570 ± 0.0293	0.9555 ± 0.0439	0.9476 ± 0.0294
Sensitivity	0.8729 ± 0.0745	0.8576 ± 0.0973	0.8536 ± 0.0608
Specificity	0.9844 ± 0.0230	0.9864 ± 0.0197	0.9754 ± 0.0286
Dice	0.8936 ± 0.0698	0.8854 ± 0.0731	0.8536 ± 0.0928
(b)			
	COVID-19	**Normal**	**Pathological**
Accuracy	0.9761 ± 0.0100	0.9801 ± 0.0104	0.9769 ± 0.0111
Sensitivity	0.9444 ± 0.0443	0.9470 ± 0.0373	0.9340 ± 0.0525
Specificity	0.9867 ± 0.0108	0.9906 ± 0.0059	0.9891 ± 0.0077
Dice	0.9447 ± 0.0241	0.9528 ± 0.0161	0.9414 ± 0.0322

References

1. Ozturk, T.; Talo, M.; Yildirim, E.A.; Baloglu, U.B.; Yildirim, O.; Acharya, U.R. Automated detection of COVID-19 cases using deep neural networks with X-ray images. *Comput. Biol. Med.* **2020**, *121*, 103792. [CrossRef] [PubMed]
2. de Moura, J.; Novo, J.; Ortega, M. Fully automatic deep convolutional approaches for the analysis of Covid-19 using chest X-ray images. *IEEE Access* **2020**, *8*, 195594–195607. [CrossRef]
3. de Moura, J.; Garcia, L.R.; Vidal, P.L.; Cruz, M.; Lopez, L.A.; Lopez, E.C.; Novo, J.; Ortega, M. Deep Convolutional Approaches for the Analysis of COVID-19 Using Chest X-Ray Images From Portable Devices. *IEEE Access* **2020**, *8*, 195594–195607. [CrossRef]
4. Moris, D.I.; de Moura, J.; Novo, J.; Ortega, M. Cycle Generative Adversarial Network Approaches to Produce Novel Portable Chest X-Rays Images for Covid-19 Diagnosis. In Proceedings of the ICASSP 2021—2021 IEEE International Conference on Acoustics, Speech and Signal Processing (ICASSP), Toronto, ON, Canada, 6–11 June 2021. [CrossRef]
5. Vidal, P.L.; de Moura, J.; Novo, J.; Ortega, M. Multi-stage transfer learning for lung segmentation using portable X-ray devices for patients with COVID-19. *Expert Syst. Appl.* **2021**, *173*, 114677. [CrossRef] [PubMed]

6. Buda, M. U-Net for Brain MRI, Pytorch Hub. 2020. Available online: https://pytorch.org/hub/mateuszbuda_brain-segmentation-pytorch_unet/ (accessed on 20 October 2020).
7. Kermany, D. Labeled Optical Coherence Tomography (OCT) and Chest X-Ray Images for Classification. Mendeley Data. 2018. Available online: https://data.mendeley.com/datasets/rscbjbr9sj/2 (accessed on 1 September 2020). [CrossRef]
8. Cohen, J.P.; Morrison, P.; Dao, L.; Roth, K.; Duong, T.Q.; Ghassemi, M. COVID-19 Image Data Collection: Prospective Predictions Are the Future. *arXiv* **2020**, arXiv:2006.11988.